

Significantly improves the mechanical strength of Aluminum alloy adhesive joint through electrochemical pretreatment in environmentally friendly medium

Zhenghui Ge^{a,*}, Qifan Hu^a, Kai Pang^b, Yongwei Zhu^a, Xiaonan Hou^b

^aCollege of Mechanical Engineering, Yangzhou University, Yangzhou 225009, China

^bDepartment of Engineering, Engineering Building, Lancaster University, Lancaster LA1 4YW, UK

*Corresponding author: Zhenghui Ge (zhge@yzu.edu.cn)

Abstract: Adhesive bonding of aluminum alloys is extensively practiced to achieve optimum lightweight and reliable structures in the aerospace, automobile, and maritime industries. This paper represents the inaugural attempt to use neutral salt solutions as electrolytes for the electrochemical pretreatment of aluminum alloy bonding surfaces, with the aim of achieving high-performance bonding. The NaNO₃ and NaCl solutions were selected carefully due to their non-toxic, easy to obtain, and inexpensive. Comprehensive experiments were conducted, and the specimen surfaces were characterized by advanced characterization methods before and after electrochemical treatment. The results demonstrated that the surface morphology of the treated aluminum alloy exhibited notable alterations, and the wettability, roughness, and chemical composition were effectively improved. Subsequently, aluminum alloy single lap joints were subjected to detailed examination in order to evaluate the effectiveness of the pretreatments on the bonding strength and fracture resistance. The results showed that under the condition of 5 A and 1 min, the specimen treated with NaCl solution demonstrated a notable enhancement in bonding performance, and its bonding strength increased by more than 200% that of the untreated specimen joints. Moreover, this study integrates the characterization and experimental findings to provide a comprehensive analysis of the mechanisms underlying the deterioration or improvement of the bonding performances under different pretreatment conditions. This study demonstrates not only the extremely friendly characteristics to operators and environment, but also the technical advantages of low cost, high efficiency and good bonding performance.

Keywords: Adhesive bonding, Aluminum alloy, Electrochemical surface treatment, Failure model, Bonding performance

1. Introduction

Adhesive bonding technology is a method of connecting components by treating their surfaces and applying adhesive to form a cohesive whole. Compared with

traditional fasteners such as bolts, rivets, and welding, adhesive bonding has technical advantages such as flexible design, easy manufacturing, and more uniform stress distribution, and has been widely used in the industrial field [1-3]. For example, in the aerospace industry, adhesive technology is a pivotal methodology employed in the fabrication of structural components, including heat shields, fuselages, and wings. Similarly, in the automotive sector, adhesive technology is a prevalent technique utilized in the construction of body structures and battery pack casings. Moreover, adhesive technology also offers an efficacious solution for the implementation of sandwich panel structures in the shipbuilding industry [4-6].

The appropriate surface treatment of the bonding surface prior to bonding is an effective means of improving bonding performances. Physical methods such as sanding, grinding, sandblasting, etc. are the most commonly used techniques of bonding surface treatment for enhancing bonding performance, and have been extensively researched by scientists [7-10]. With the development of surface treatment technology, the means of surface treatment have become increasingly diverse. In recent years, various forms of surface treatment techniques have emerged one after another, including laser [11-13], chemical etching, plasma [14-17], nano-enhancing [18,19], surface topology [20], etc., and have been extensively studied.

Among these methods, chemical treatment stands out due to its technical advantages such as simple process, easy operation, and no need for expensive processing equipment, which has attracted widespread attention from both industry and academia. Chemical etching represents a widely utilized chemical treatment method for the surface pretreatment of aluminum alloys. Hu et al. investigated the etching effect of different concentrations of NaOH solutions in an ultrasonic bath at 55°C to obtain the optimum wettability and roughness of the aluminum alloy surfaces [21]. The study, conducted by Saleema et al., undertook a comprehensive investigation into the influence of time on surface etching in an ultrasonic bath of NaOH solution. Their findings indicated that a minimum of 30 minutes was required for the treatment to induce the rough evolution of the microstructure of the aluminum surface. Finally, by optimizing the treatment time, a rough micro-surface texture was obtained, resulting in

an increase in bonding strength of approximately 60% [22]. Mahfoudh et al. employed a combination of NaOH etching and mixed solution of sulfuric acid and iron sulfate to treat aluminum alloy joints [23]. The findings demonstrated that, in comparison to NaOH treatment alone, the combination treatment approach resulted in an approximately 60% enhancement in the fracture energy. Prolong et al. explored the effect of acidic mixed solution etching on bonding performances and found that specimens treated with a mixture of 10% sulphonic acid and 20% ferric sulphate at 65°C gave better bonding strength [24]. Shokriani et al. examined the impact of diverse acidic solutions and their combination methods on the bonding performance. Their findings revealed that the combination methods of 25 min in hydrochloric acid solution and 40 min in nitric acid solution resulted in the highest values of cohesion destruction [25]. The aforementioned report indicates that chemical etching methods can effectively enhance the bonding performances of aluminum alloy joints. However, chemical etching also presents certain challenges, including prolonged processing times, the potential for injury to personnel and environmental pollution.

Anodizing is the most prevalent and widely accepted surface pretreatment technique for aluminum alloys. H_2CrO_4 and H_3PO_4 are the electrolytes most commonly used in the anodizing process, this is due to their ability to produce porous oxide films with higher porosity [26,27]. For example, Zhang et al. effectively enhanced the bonding strength of aluminum alloy by anodic oxidation in H_2CrO_4 baths. They pointed out that this was due to the formation of a porous oxide layer on the aluminum alloy surface by anodic oxidation, which enhanced the mechanical interlocking between the adhesive and the aluminum alloy specimen accordingly [28]. Chen et al. conducted anodizing treatment on aluminum alloys in H_3PO_4 baths. They proposed that phosphoric acid anodizing can form a porous microstructure and larger roughness on the surface of aluminum alloys. This, they suggest, leads to the resin melt flying into the nanopores, thereby forming micro mechanical interlocking [29]. Dong et al. modified the fracture mode of the SLJs between aluminum alloy and thermoplastic polyether ether ketone adhesive by optimizing the anodizing treatment parameters in H_3PO_4 solution. Moreover, they underscored that the creation of an adequate number

of circular structural pits on the aluminum alloy surface through anodizing represents a pivotal step in augmenting the bonding strength [30]. However, studies have also shown that types of anodizing baths such as H_2CrO_4 and H_3PO_4 are extremely environmentally unfriendly, and even release carcinogens during the anodizing process, which could have a significant adverse impact on human health [31,32]. In recent years, scholars have begun to search for electrolytes that can ensure effective bonding strength while also being environmentally friendly. Correia et al. conducted research on anodizing surface pretreatment using four different electrolyte solutions. Through extensive experiments, it was determined that sulfuric acid and boric-sulfuric acid represented the optimal alternative to anodizing medium for aluminum alloy surfaces [33]. In the study conducted by Fiore et al., anodizing was performed in a tartaric sulfuric acid solution. The bonding strength was found to have increased by approximately 50-60% when specimens were compared with those that had undergone mechanical grinding [32]. Nevertheless, the anodizing process, which involves the use of an acidic solution, has been identified as an environmentally unfriendly practice. Additionally, the process has been found to have shortcomings, including prolonged consumption times and limited enhancement in the bonding performance of aluminum alloy specimens when employed as a standalone technique.

On the other hand, numerous have conducted research on the surfaces pretreatment of aluminum alloy specimens by multi-process combination methods, with the objective of enhancing the bonding performance of aluminum alloy SLJs. Akpinar initially subjected the aluminum specimen to a chemical treatment with NaOH solution, and later anodized it in H_3PO_4 solution to obtain better roughness and surface properties. Subsequently, an epoxy pre-coating comprising carbon nanotubes (CNT) was applied to the anodized surface, resulting in a 93% increase in joint strength [34]. Zhang et al. first ultrasonically cleaned the aluminum alloy specimens with acetone and treated it with NaOH solution to remove some surface stains and insoluble substances. After cleaning with HNO_3 and deionized water, the aluminum alloy specimens were anodized in a mixture solution of H_2SO_4 , H_3PO_4 , and $\text{H}_2\text{C}_2\text{O}_4$ for 30 minutes. The experimental results showed that the aluminum specimens treated by the composite process changed

from interfacial debonding failure to cohesive failure [35]. Cheng et al. carried out anodizing in a mixture solution of H_2SO_4 , and $H_2C_2O_4$ for more than 60 min to obtain deep grooves on the aluminum surface with a depth of up to 5 μm . A resin/acetone mixture containing CNT was subsequently applied to the bonding surface, and the bonding strength was observed to have increased by 135.2% as a consequence of the embedding of CNT into the aforementioned grooves [36]. Nasreen et al. employed a solution of NaOH to remove contaminants from the metal surface. This was followed by chemical etching in a mixture solution of H_2SO_4 , H_2O and $Na_2Cr_2O_7$. Finally, anodizing was carried out in H_3PO_4 solution. The results demonstrated that this combined process resulted in an increase in stiffness performance of the SLJs by up to 36% [37]. The aforementioned methods demonstrate that a combination of pretreatment methods can fully leverage the technical advantages of the various pretreatment techniques and further enhance the bonding potential of aluminum alloy joints. Nevertheless, the combination of pretreatment methods is complex and appears to require greater investment of time and resources.

With the rapid development of modern industry, there is an urgent need to develop a surface pretreatment method that offers the advantages of high efficiency, low cost, superior bonding quality and environmentally friendly. This paper represents an inaugural attempt to use neutral salt solutions as electrolytes for the electrochemical pretreatment of aluminum alloy specimen surfaces, and high-performance bonding was successfully achieved. Numbers of characterization techniques were employed to observe alterations in the properties of aluminum specimen surfaces, including surface morphology, roughness, wettability and chemical composition, both before and after electrochemical treatment. The underlying mechanism of the deterioration or improvement of bonding performances under varying pretreatment conditions were elucidated. The findings of this study illustrate that the electrochemical pretreatment method in neutral salt solution has many beneficial properties, including being extremely operator and environmentally friendly, as well as offering technical advantages in terms of low cost, high efficiency and good bonding.

2. Experimental

2.1. Material

In order to accurately evaluate the impact of electrochemical treatment on the interface properties, the two adherend materials of the joints were uniformly selected the same material. Aluminum alloy 6082-T6 is widely used in the automotive and aerospace industries for products such as body structures, fuselage, and wings due to its low density, high strength and excellent machinability [38,39]. In addition, aluminum alloy 6082-T6 is also used to make sandwich panels for greater lightweighting purposes [40]. Therefore, aluminum alloy 6082-T6 was specifically employed in this study. The chemical compositions of AA 6082-T6 as listed in Table 1 and was provided by the manufacturer. Loctite EA 9497 was used as adhesive, which is a medium viscosity, two-component room temperature curing epoxy. Tensile tests were carried out for both adherend and adhesive materials based on the ISO EN 485-2:2016 and ISO 527-2 respectively, and their mechanical properties are shown in Table 2.

Table 1

Chemical composition of untreated AA6082-T6.

Material	Elemental composition (Wt%)								
	Si	Fe	Cu	Mn	Mg	Zn	Ti	Cr	Al
AA6082-T6	0.82	0.22	0.02	0.53	0.64	0.02	0.01	0.01	97.73%

Table 2

The bulk property of adherends and adhesives [41,42].

Property	Al 6082	Loctite EA 9497
Young Modulus (MPa)	70770±385	7705.35±468.08
Yield Stress (MPa)	254.59±3.20	46.29±3.13
Elongation at fracture (%)	10.83±0.95	0.71±0.09
Poisson Ratio	0.30±0.01	0.29
Density (tonne/mm ³)	2.7±10 ⁻⁹	1.1±10 ⁻⁹

2.2. Electrochemical treatment parameter and strategy

The electrochemical treatment process is shown in Fig. 1, including aluminum specimens, stainless steel electrode, shielding plate and medium solution, etc. The

aluminum specimens and the stainless-steel electrode are simultaneously placed in a solution cell filled with processing medium and connected to the positive and negative poles of an external power supply, respectively. The insulating shielding plate is employed to cover the areas of the aluminum specimens that do not require treatment, thereby exposing only the bonding areas that are to be treated. This approach facilitates the objective of localized electrochemical treatment.

To avoid any health and environmental concerns, neutral salt solutions were chosen as the treatment medium in this paper. 10% concentration NaNO_3 solution and NaCl solution were carefully selected, they are inexpensive and easy to obtain. The external power supply selects constant current mode, with 1 A and 5 A applied separately, and the entire electrochemical treatment time is set to 1 minute. All specimens were washed three times before and after electrochemical treatment using water-alcohol-water alternation to maximize the removal of surface grease spots and impurities. The detailed electrochemical treatment strategy is shown in [Table 3](#).

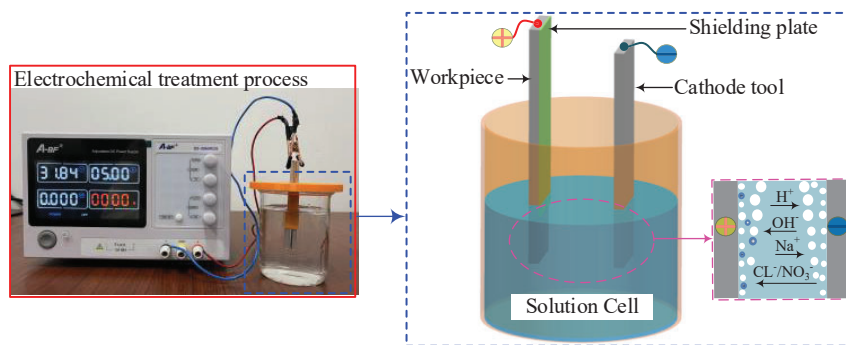


Fig. 1. Schematic diagram of electrochemical treatment process.

Table 3

Single-lap joint configuration for testing.

ID	Property	Current (A)	Time (s)	Treatment area (mm ²)
Model-1	untreated	/	/	/
Model-2	10% NaCl	1	60	25×25
Model-3	10% NaCl	5	60	25×25
Model-4	10% NaNO_3	1	60	25×25
Model-5	10% NaNO_3	5	60	25×25

2.3. Surface characteristics analysis

The surface of the specimen was characterized using a scanning electron

microscope (SEM, GeminiSEM 300 FESEM, Carl Zeiss Microscopy GmbH, Germany), and the chemical composition of the specimen surface was analyzed using energy-dispersive X-ray spectroscopy (EDX). The surface roughness of the specimen was characterized by 3D measurement laser microscope (LEXT OLS5000 Laser, Olympus, Japan). The contact angle (CA) of water droplets on the specimen surface was determined after a period of 1 minute using the contact angle measuring system (ZJ-7000, Shenzhen, China) at room temperature. Three measurements were taken for each specimen surface with a droplet volume of 2 μL of distilled water and diiodomethane as the experimental droplets.

The small CA indicates that, for a given volume of liquid, the liquid will expand more over the surface, which is indicative of the liquid having a high degree of wettability to that surface. Conversely, the large CA indicates a lower degree of wettability. In this paper the surface free energy (SFE) of aluminum specimens were calculated using the Owens-Wendt-Rabel-Kaelble (OWRK) method, which divides the SFE of a solid into a disperse and a polar component. The values and parameters of the SFE are shown in [Table 4](#).

$$\gamma_S = \gamma_S^D + \gamma_S^P \quad (1)$$

where γ_S is the solid SFE; γ_S^D is the dispersion component of the solid SFE; γ_S^P is the polar component of the solid SFE. Values of γ_S^D and γ_S^P are calculated from Eqs. (2) and (3).

$$\gamma_{LW} (1 + \cos \theta_W) = 2 \left(\gamma_S^D \gamma_{LW}^D \right)^{\frac{1}{2}} + 2 \left(\gamma_S^P \gamma_{LW}^P \right)^{\frac{1}{2}} \quad (2)$$

$$\gamma_{LD} (1 + \cos \theta_D) = 2 \left(\gamma_S^D \gamma_{LD}^D \right)^{\frac{1}{2}} + 2 \left(\gamma_S^P \gamma_{LD}^P \right)^{\frac{1}{2}} \quad (3)$$

where γ_{LW} is the SFE of water; θ_W is the measured CA of water; γ_{LW}^D is the disperse component of the water SFE; γ_{LW}^P is the polar component of the water SFE; γ_{LD} is the SFE of diiodomethane; θ_D is the measured CA of diiodomethane; γ_{LD}^D is the disperse component of the diiodomethane SFE; γ_{LD}^P is the polar component of the diiodomethane SFE.

Table 4

Surface tension components of the test liquids (mJ/m^2).

Liquid	γ_L	γ_L^D	γ_L^P
Water	72.8	21.8	51
Diiodomethane	50.8	50.8	0

The chemical elements and composition of the outermost layer on the surface of the aluminum alloy specimens before and after electrochemical treatment were determined by X-ray photoelectron spectroscopy (XPS, ESCALAB 250Xi, Thermo Fisher Scientific Inc., USA). Under the constant analyzer energy (CAE) mode, a measurement spectrum was obtained with an energy setting of 100 eV and an energy step of 0.1 eV. In this experiment, each specimen underwent narrow scan spectral analysis, a method that enables the quantitative assessment and interpretation of the chemical states of various elements. By calculating the peak areas of the spectra and considering sensitivity factors, the percentage composition of different elements on the specimen surface was determined. The test results were then analyzed using Avantage software. Prior to curve fitting, a binding energy calibration was performed for the non-degenerate hydrocarbon at a binding energy of 284.8 eV.

2.4. Joint configuration and fabrication

In this study, five different types of Single Lap Joints (SLJs) were carefully manufactured, which are labelled as follows: untreated (Model-1), NaCl-1A (Model-2), NaCl-5A (Model-3), NaNO₃-1A (Model-4) and NaNO₃-5A (Model-5), as shown in [Table 3](#). All the five types of SLJs were manufactured with identical values of the length of adherends ($L = 100$ mm), the thickness of adherends ($t_s = 3$ mm), the thickness of the adhesive ($t_a = 0.2$ mm) and joint's width ($W = 25$ mm) and the overlap length of ($L_s = 25$ mm), as shown in [Fig. 2](#). The square tabs with a dimension of $L_t = 25$ mm were bonded at the end of the joints to secure correct alignment in the testing machine. The untreated specimen, which had not undergone any surface modification treatment and was only washed three times using water-alcohol-water alternation prior to bonding, was used to fabricate the SLJs (Model-1). Then the SLJs (Model-1) was employed as the reference model for comparison with the modified SLJs, with the objective of elucidating the advantages of the electrochemical treatment technique in the bonding area.

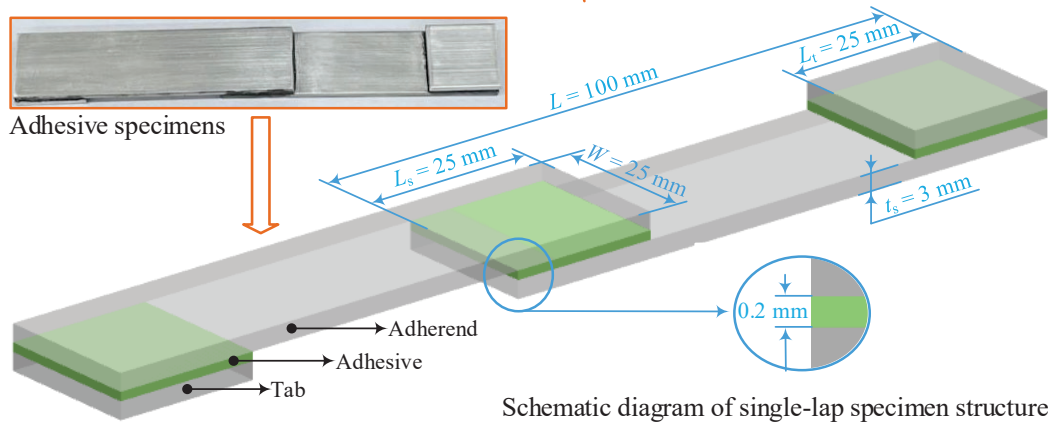


Fig. 2. Dimensions and geometry of SLJs in this study.

All tensile tests were carried out using Instron 3380 with a 100 kN load cell. The loading was under displacement control at a speed of 0.5 mm/min. At least five specimens of each joint type were continuously loaded till the final failure. Non-contact optical method (Imetrum system) was used to measure displacement and observe the failure process in SLJ tests (Fig. 3). All SLJs were masked with white background and black dots with a diameter of 0.3 mm to create speckle patterns on the lateral surface of SLJs. The camera then tracked the dots and the first pattern was used as the reference image, to which other images were compared. When calibrating the dimension for the camera, the paper rule was used.

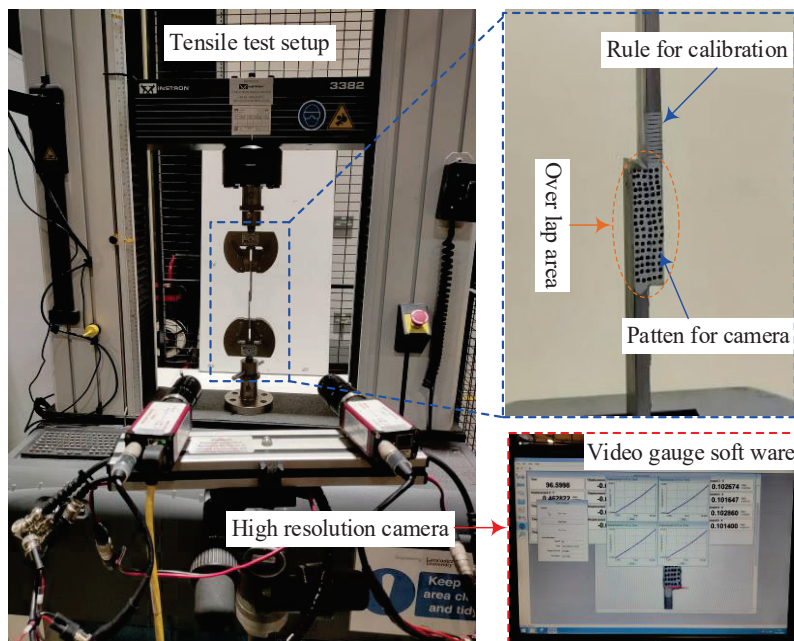


Fig. 3. The tensile test setup for an SLJs with a non-contact measurement system.

3. Results and discussion

3.1 Surface morphology and elemental analysis

Fig. 4 illustrates the surface morphology and elemental composition of the untreated surface and the electrochemical treated surfaces under various conditions. The presence of parallel texture on the untreated surface is clearly discernible (Fig. 4(a)), and it can be established that these were created during the extrusion process. The EDX results indicate the presence of elemental oxygen in addition to the elemental aluminum. Given the sensitivity of aluminum alloys to oxidation in air, it can be inferred that an oxide layer structure is present on the untreated surface. Furthermore, the presence of carbon elements was also identified, which may be indicative of contaminants generated during the handling, storage, and transportation processes, given the relatively low carbon content observed in the aluminum substrate. The treated surfaces in NaNO_3 solution display a distinctive blackening phenomenon, which becomes increasingly pronounced with the increase of current (Fig. 4(b) and (c)). The SEM images illustrate that the initial texture persists on the surface of the treated specimen with conditions of NaNO_3 solution and 1 A, indicating that the initial oxide layer has not been entirely destroyed. Conversely, the initial texture has been entirely removed at 5A, and the surface of the treated specimen displays some fissure-like tissue. The EDX analysis indicates that the surface oxygen content increases following electrochemical treatment, particularly at 5A, where the surface oxygen content reaches as high as 8.12%. This phenomenon can be described as a rapid dissolution of the initial oxide layer structure on the untreated surface under high current conditions of 5A. However, the electrochemical treatment products adhere to the aluminum substrate surface in the NaNO_3 solution, thereby forming a new loose corrosion layer.

Unlike the effect of NaNO_3 solution, there was no significant color change on the specimen surface treated with NaCl solution (Fig. 4(d) and (e)). The SEM image illustrates that at 1A, the initial surface texture begins to dissolve, while at 5A, the initial surface texture has been completely removed, and there are no discernible residual fissure-like tissues on the surface. This can be attributed to the fact that chloride ions have more pronounced destructive effect on the surface oxide layer of aluminum alloys than nitrate ions. It can be concluded that the electrochemical treatment products are

less likely to adhere to the aluminum substrate surface in NaCl solution [43]. Furthermore, the EDX results indicated that at 5A, the oxygen content remained relatively consistent with the untreated surface, whereas the carbon content exhibited a notable decline. This suggests that the initial oxide layer on the untreated surface is rapidly dissolved and a new dense oxide layer structure is formed, which is completely different from the loose corrosion layer structure that forms on the aluminum substrate surface in NaNO₃ solution at 5A.

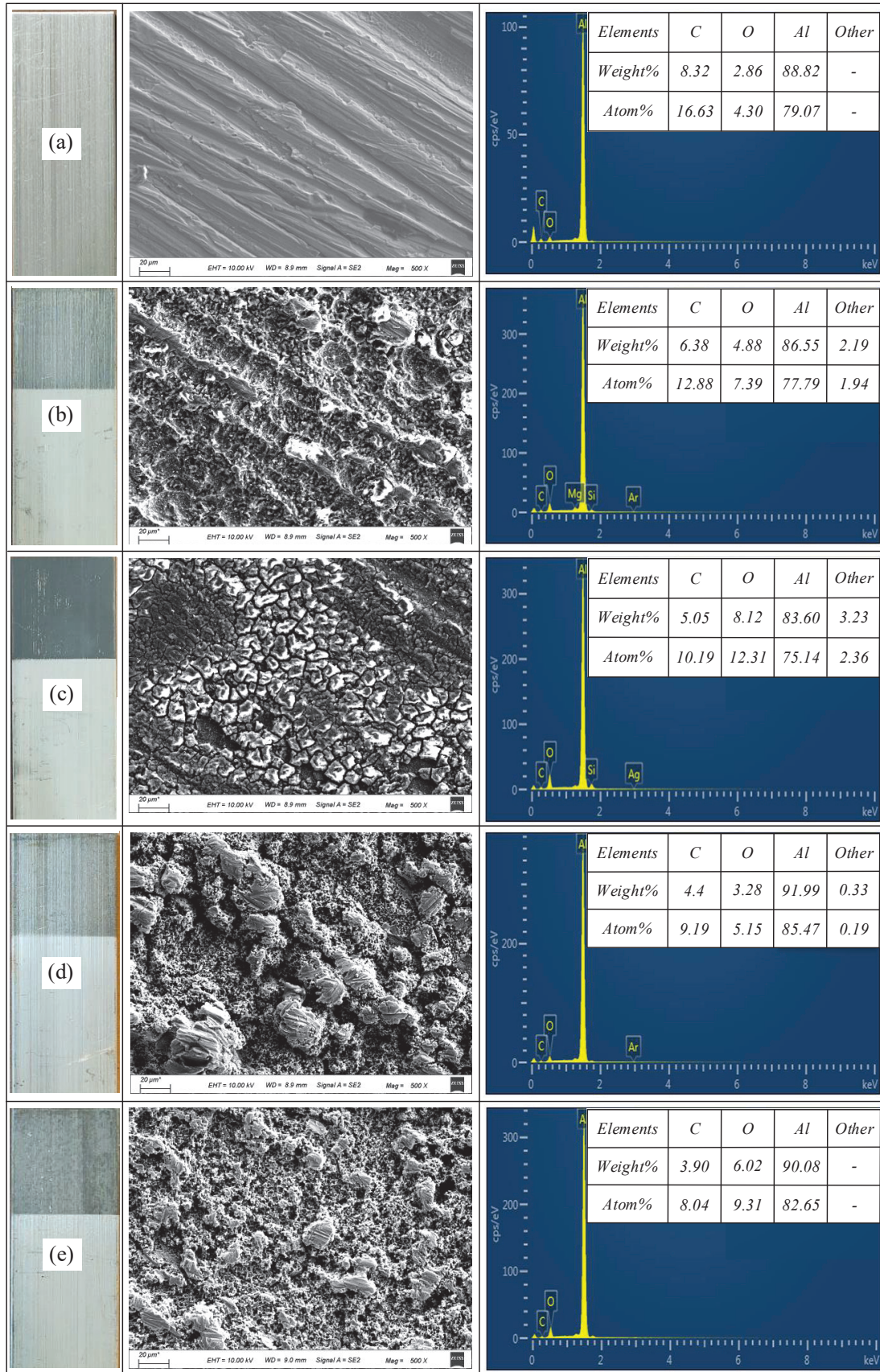


Fig. 4. Surface morphology and elements analysis of aluminum alloy specimens, (a) untreated and treated by (b) 1 A in NaNO₃ solution, (c) 5 A in NaNO₃ solution, (d) 1 A in NaCl solution, (e) 5 A

in NaCl solution.

3.2. Surface chemical composition analysis

The XPS survey spectra of the aluminum specimens is shown in Fig. 5. Elements such as Al, O, C, Si, Mg and Cu were detected (Fig. 5(a)), and all these elements except C and O are essential components of the AA6082-T6 aluminum alloy as shown in Table 1. It is hypothesized that the C 1s peak is the result of surface contamination. While the presence of O 1s peak can be attributed to organic contaminants, it can also be attributed to a significant extent to the oxide layers on the aluminum substrate.

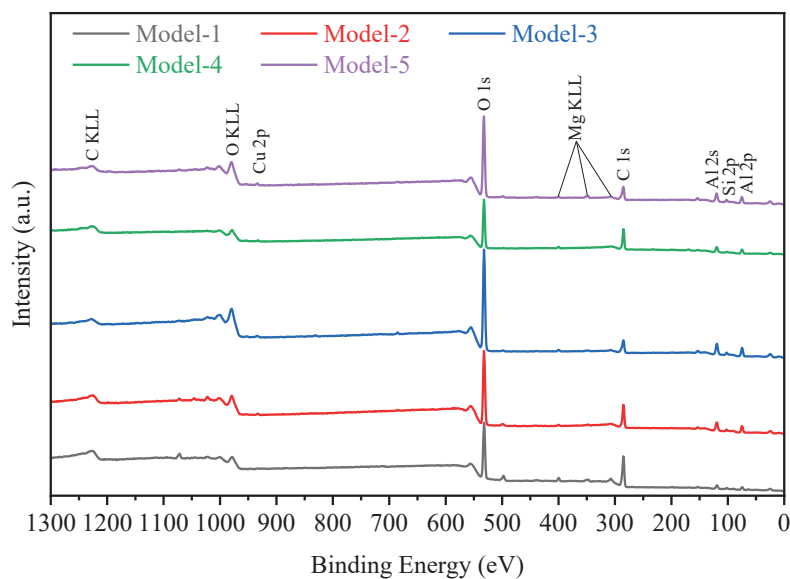


Fig.5. Survey spectra of the AA6082-T6 aluminum alloy surfaces.

To further analyze the surface chemical components, high-energy resolution XPS spectra of C 1s, Al 2p and O 1s of the untreated surface and the electrochemical treated surfaces are represented in Fig. 6. Further peak fitting analysis showed that the C-C(H) on the electrochemical treated surfaces was significantly reduced compared to the untreated surface, as shown in Fig. 6(a)-(e). This suggests that the contaminants present on the untreated surface may be predominantly in the form of C-C(H) and that these contaminants can be effectively removed by the electrochemical treatment method [44]. Moreover, comparison of the C-C(H) content of specimens subjected to electrochemical treatment at different currents revealed that the C-C(H) content at 5A was markedly lower than that at 1A, regardless of whether the solution was NaNO_3 or NaCl. This can be interpreted as most of the contaminants adhering to or penetrating

the surface layer of the untreated alloy. As the aluminum alloy surface material is gradually dissolved by electrochemical treatment, there is a corresponding decrease in the surface carbon content.

The aluminum hydroxide content on the electrochemical treated surfaces is significantly increased in comparison to the untreated surface (Fig. 6(f)-(j)). This phenomenon can be attributed to the gradual dissolution of aluminum ions on the untreated surface during electrochemical treatment. These aluminum ions combine with hydroxide ions present in the electrolyte to form aluminum hydroxide, which then adheres tightly to the surface of the aluminum alloy specimens. It is worthy of note that aluminum hydroxide is considered to display superior hydrophilic properties in comparison to aluminum oxide [21]. Therefore, it can be inferred that the bonding strength of the aluminum alloy specimens subjected to electrochemical treatment may be considerably greater than that of the untreated aluminum alloy specimens. On the other hand, whether it is NaNO₃ solution or NaCl solution, the aluminum hydroxide content of electrochemical treatment surfaces at 5A is higher than that of the electrochemical treatment surfaces at 1A. Moreover, compared with aluminum hydroxide content of untreated surfaces, the aluminum hydroxide content of the electrochemical treatment surfaces at 5A has significantly improved. This not only indicates that the surface structure of the electrochemical treated specimens at 5A has been significantly changed from the untreated specimens, but also indicates that electrochemical treatment at high currents may be beneficial to obtain stronger bonding performances. However, considering the loose corrosion layer structure observed on the electrochemical treated surface with conditions of NaNO₃ solution at 5A and the denser oxide layer structure observed on the electrochemical treated surface with conditions of NaCl solution at 5A, discussed in Section 3.1 and 3.2. It can be hypothesized that the electrochemical treated specimens with conditions of NaCl solution and 5A may demonstrate exemplary bonding performances, given that the bonding strength between the loose corrosion layer of the electrochemical treated specimens in NaNO₃ solution and 5A and the aluminum substrate may be disrupted (Fig. 3(c)).

The examination of high-energy resolution XPS spectra of the O 1s element revealed an increase in the content of oxides on the electrochemical treated surfaces in comparison to the untreated surface (Fig. 6(k)-(o)). This phenomenon may be attributed to the formation of aluminum oxide and aluminum hydroxide on the surface of the electrochemical treated specimens. As we know, both aluminum oxide and aluminum hydroxide demonstrate excellent stability at room temperature and are resistant to dissolution or removal, thereby maintaining a high oxygen content on the electrochemical treated specimen surface. The formation of a new aluminum hydroxide and aluminum oxide layer may serve to enhance the bonding strength between the adhesive and the surface of the aluminum alloy specimens [45]. Furthermore, the figure also demonstrates that the oxygen content at 1A is markedly lower than that at 5A, despite the identical solution conditions. This phenomenon can be attributed to the insufficient electrochemical effect at 1A, which results in inadequate reaction activity on the aluminum alloy surface, thereby leading to a lower amount of oxide or hydroxide generation than at 5A.

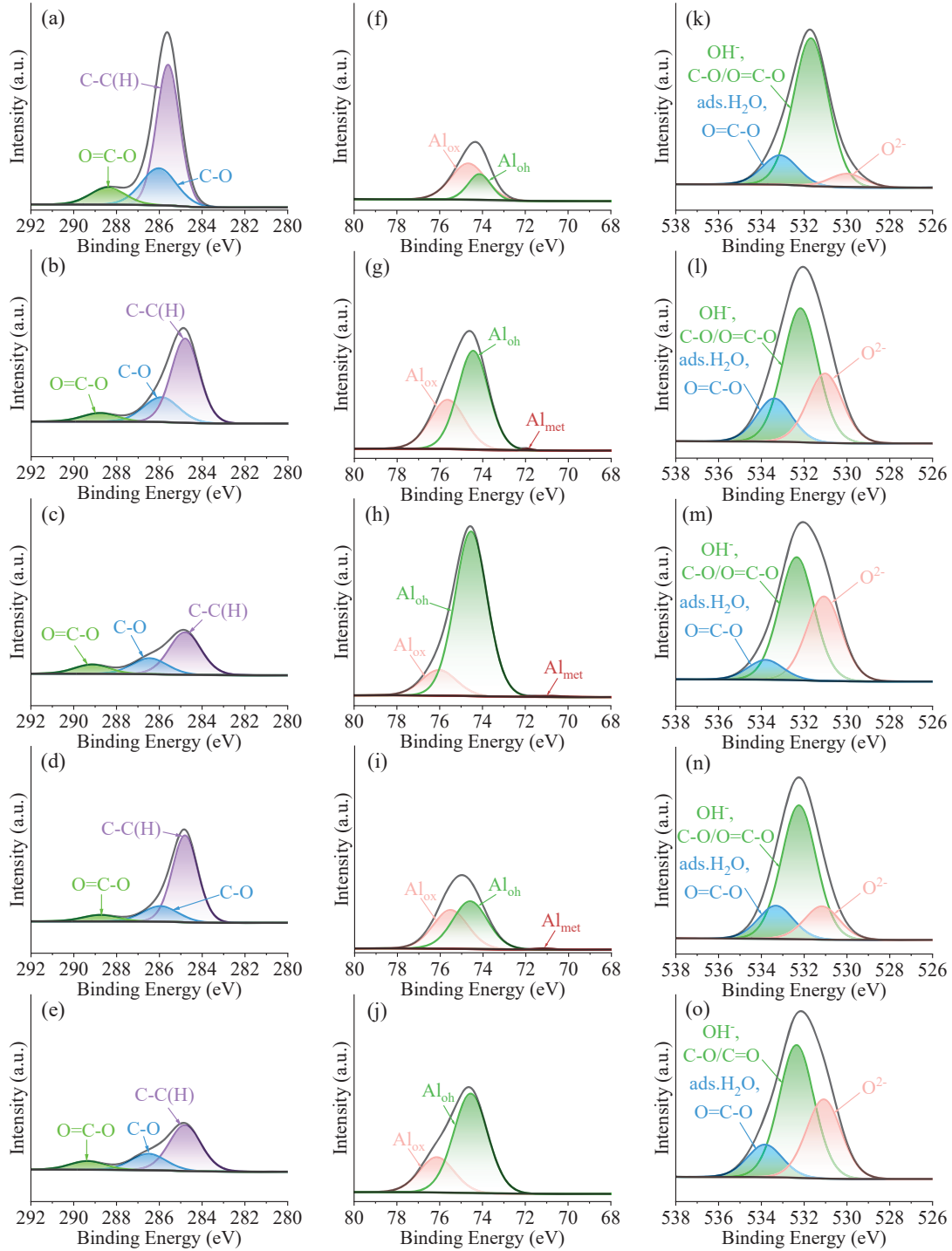


Fig. 6. High resolution spectra of (a)-(e) C 1s, (f)-(j) Al 2p and (k)-(o) O 1s for (a),(f) and (k) Model-1, (b), (g) and (l) Model-2, (c), (h) and (m) Model-3, (d), (i) and (n) Model-4, (e), (j) and (o) Model-5.

3.3 Surface roughness analysis

In this section, five 3D surface roughness parameters, including S_a (arithmetic mean deviation of the surface), S_z (maximum height of the surface), S_p (maximum peak height of the surface), S_v (maximum valley depth of the surface), and S_{dr} (interface

expansion area ratio), were employed to characterize the morphology of the untreated surface and electrochemical treated surfaces, as shown in [Table 5](#). The surface roughness of the untreated specimen, which reaches a value of 2.886 μm , can be attributed to the presence of surface parallel textures. Following electrochemical treatment, a transformation was observed in the three-dimensional morphology of the specimen surface. The degree of this transformation was found to be closely related to the applied current, with greater degrees of transformation occurring at higher current densities. As illustrated in [Table 5](#), the surface textures remain visible under condition of 1A irrespective of whether the solution is NaCl or NaNO₃. Similarly, the surface roughness also demonstrates minimal variation from the untreated surface. This further corroborates the hypothesis that the surface oxide layer of the untreated specimen was not entirely removed under the condition of 1A, as discussed in [Section 3.1](#). In contrast, under the condition of 5A, the surface texture has entirely removed, irrespective of whether the solution is NaCl or NaNO₃. However, there are significant differences in the surface morphology characteristics of different solution at 5 A.

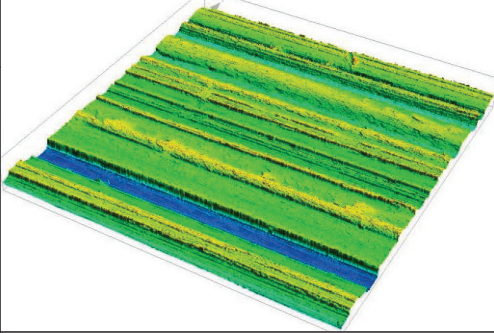
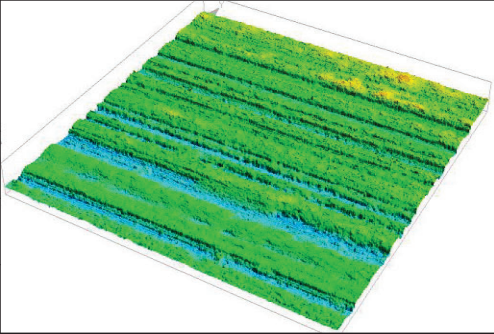
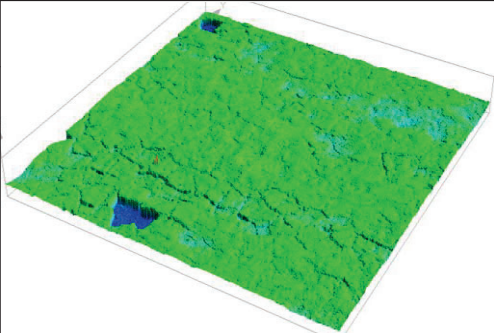
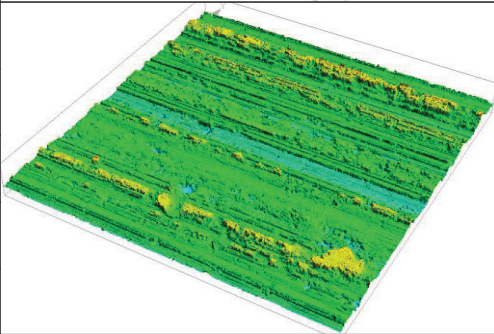
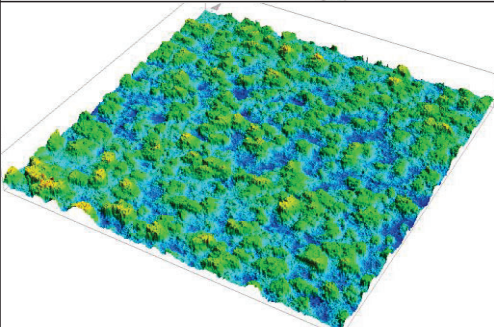
The surface treated with NaNO₃ solution is relatively smooth, and its S_a significantly decreases to 1.749 μm . This is due to the fact that NaNO₃ solution is a typical passivating electrolyte, which will locally corrode the texture raised areas of untreated surface during electrochemical treatment. Conversely, the texture depressed areas on the untreated surface are rarely or never corroded, thus achieving the effect of reducing the surface roughness. It is noteworthy that while the S_a of the surface treated with NaNO₃ solution decreased significantly by 40% in comparison to the untreated surface, the values of S_z , S_p , S_v slightly increased. In light of the preceding discussions in [Sections 3.1 and 3.2](#), it can be reiterated that a corrosion layer is present on the surface of the aluminum substrate in NaNO₃ solution, with the specific parameters being 5A. Moreover, the corrosion layer is relatively loose, comprising numerous micropores and microcracks, as observed in [Fig. 4\(c\)](#). This may facilitate adhesive penetration and thus improve the bonding strength. Conversely, if the bonding force at the interface between the corrosion layer and the aluminum substrate is insufficient, it may result in a reduction in the overall bonding strength of the joints. This is due to the potential

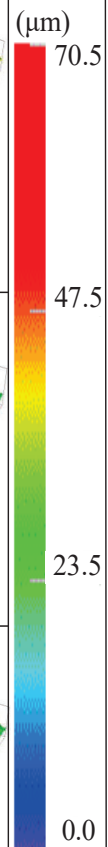
fracture of the bonding interface between the corrosion layer and the aluminum substrate.

In contrast to the effect of NaNO₃ solution, the S_a of surface treated with NaCl solution exhibits a notable increase. This is due to the fact that NaCl solution is a non-passivating electrolyte which will corrode both the raised and recessed areas of the untreated surface. This makes it difficult to level the untreated surface texture. This is consistent with existing reports of high surface roughness of corroded specimens at low current densities in NaCl solutions [46]. Furthermore, the S_{dr} of electrochemical treated surface with NaCl solution and 5A exhibited a notable increase, reaching the highest value for all specimens. The S_{dr} value of electrochemical treated specimen increased from 25.817 % under NaNO₃ solution to 69.185 % under NaCl solution. These findings indicate that the surface of electrochemical treated specimen with the NaCl solution and 5 A may exhibit a more pronounced mechanical locking effect, attributable to a notable enhancement in surface roughness and surface extension area.

Table 5

Surface roughness and 3D morphology of aluminum alloy specimens.

Adherend	Surface roughness		3D Imagine	
Model-1	S_a (μm)	2.886		
	S_z (μm)	40.375		
	S_p	21.175		
	S_v	19.112		
	S_{dr} (%)	37.082		
Model-2	S_a (μm)	2.474		
	S_z (μm)	32.146		
	S_p	17.874		
	S_v	14.259		
	S_{dr} (%)	37.957		
Model-3	S_a (μm)	1.749		
	S_z (μm)	49.346		
	S_p	25.274		
	S_v	24.159		
	S_{dr} (%)	25.817		
Model-4	S_a (μm)	2.749		
	S_z (μm)	46.656		
	S_p	21.248		
	S_v	25.407		
	S_{dr} (%)	51.135		
Model-5	S_a (μm)	4.052		
	S_z (μm)	59.446		
	S_p	32.212		
	S_v	27.274		
	S_{dr} (%)	69.185		



3.4 Surface wettability analysis

Fig. 7 shows the images of liquid drops on aluminum specimen surface before and after electrochemical treatment. Overall, the CA of distilled water and diiodomethane on the specimen surface exhibited a notable reduction following electrochemical treatment in comparison to the untreated surface. This phenomenon may be attributed to observed increase in SFE of the specimen surface following electrochemical treatment, as shown in Table 6. In the table, the value of γ_s is calculated using Eq. (1), while the values of γ_s^D and γ_s^P are calculated using Eqs. (2) and (3), respectively. A review of the existing literature reveals that the SFE of the specimen surface has a significant influence on the bonding force between the liquid and the specimen [47]. An increase in the SFE of the specimen surface results in a stronger attraction between the molecules of the liquid and the specimens. The SFE of the aluminum specimens subjected to electrochemical treatment in this paper all exhibited a notable increase, which suggests that the electrochemical treatment method may have a beneficial effect on the bonding performances of SLJs.

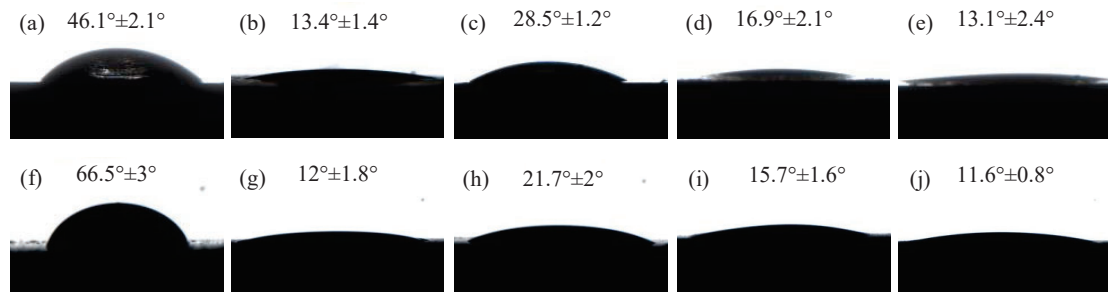


Fig.7. The CA of (a)-(e) water, (f)-(j) diiodomethane on (a) and (f) Model-1, (b) and (g) Model-2, (c) and (h) Model-3, (d) and (i) Model-4, (e) and (j) Model-5.

It is interesting to note that under the condition of 1 A, the CA of the specimens treated with NaNO_3 solution (the CA of water and diiodomethane are 13.4° and 12° respectively, as shown in Fig. 6(b) and (g)) are smaller than that of the specimens treated with NaCl solution (the CA of water and diiodomethane are 16.9° and 15.7° respectively, as shown in Fig. 6(d) and (i)). This may be attributed to the observation that the specimen surface treated with NaNO_3 solution exhibits a higher content of aluminum hydroxide, given that aluminum hydroxide is considered to be a more hydrophilic substance [21]. On the contrary, under the condition of 5A, the CA of the

specimen surface treated with NaNO₃ solution (the CA of water and diiodomethane are 28.5 ° and 21.7 ° respectively, as shown in Fig. 6(c) and (h)) are greater than that of the specimen surface treated with NaCl solution (the CA of water and diiodomethane are 13.1 ° and 11.6 ° respectively, as shown in Fig. 6(e) and (j)). This phenomenon can be attributed to the fact that the wettability of the specimen surface is influenced by a number of factors. The CA is inversely proportional to the surface roughness under conditions of good wettability of the specimen surface. Consequently, an increase in the roughness of a hydrophilic surface will result in a corresponding enhancement of its hydrophilic properties [48]. In conjunction with Table 5, the surface roughness of the electrochemical treated specimen under the conditions of NaCl solution and 5 A (S_a 4.052 μm) is markedly greater than that of electrochemical treated specimen under the conditions of NaNO₃ solution and 5 A (S_a 1.749 μm). This can be regarded as the primary factor contributing to the larger CA observed in the specimen surface treated with the NaNO₃ solution relative to the specimen surface treated with the NaCl solution under the condition of 5 A. In addition, it is noteworthy that the electrochemical treated specimen with NaCl solution and 5 A exhibited a particularly pronounced improvement in surface wettability, with the CA of water and diiodomethane being the smallest of all the specimens. Meanwhile, the electrochemical treated specimen with NaCl solution and 5 A also had the highest surface roughness among all specimens. It can thus be postulated that the electrochemical treated specimen with NaCl solution and 5 A may achieve the highest bonding strength due to the compounding effect of good surface wettability and high roughness.

Table 6

The OWRK method was used to derive γ_s^D , γ_s^P and γ_s (mJ/m²) values for aluminum under different conditions.

Treatments	γ_s^D	γ_s^P	γ_s
Model-1	24.8	28.9	53.7
Model-2	49.7	29.7	79.4
Model-3	47.3	25.8	73.1
Model-4	48.9	29.2	78.1
Model-5	49.8	29.7	79.5

3.5 Joints strength analysis

Fig. 8 demonstrates the results obtained from SLJs tests, where Fig. 8(a) is the average shear strength of various SLJs and Fig. 8(b) is the representative load-displacement curves. The electrolyte solution exerts a considerable influence on the bond strength of aluminum alloy specimens subjected to electrochemical treatment. The electrochemical treated specimens in NaCl solution have a significant positive effect on the bonding strength. In particular, the average shear strength and average maximum load of the SLJs (Model-5) made from the electrochemical treated specimens with NaCl solution and 5A reached approximately 9.35 MPa and 5841 N, respectively. These values are more than 200% higher than that of the SLJs (Model-1) made from the untreated specimens. The considerable enhancement can be ascribed to a notable rise in surface roughness, which amplifies the effective bonding area of the SLJs [49]. As illustrated in Table 5, the S_a of the untreated specimen is 2.886 μm , whereas the S_a of the specimen treated under NaCl solution and 5A increased significantly to 4.052 μm . However, research has also demonstrated that excessive roughness markedly elevates surface irregularities, which can readily result in inadequate surface wetting due to its proclivity to entrap bubbles [50]. This may have a significant adverse effect on the bonding performance of the joints. It is encouraging to note that the study in Section 3.4 revealed a notable enhancement in the surface wettability of the aluminum alloy specimens following electrochemical treatment, particularly under conditions of 5A and NaCl solution, where the CA reached its minimum and the SFE reached its maximum, in comparison to all the other aluminum alloy specimens. This phenomenon serves to effectively mitigate the adverse effects of excessive surface roughness, which has the tendency to trap air bubbles and thereby impair the bonding performance of the joints. Therefore, the potential for an enhanced bonding area and a more robust mechanical locking effect, resulting from the considerable increase in surface roughness observed in the electrochemical treated surface under conditions of 5A and NaCl solution, was fully realized. This can be regarded as the primary factor contributing to the significant enhancement in the maximum load observed for Model-5 in this section.

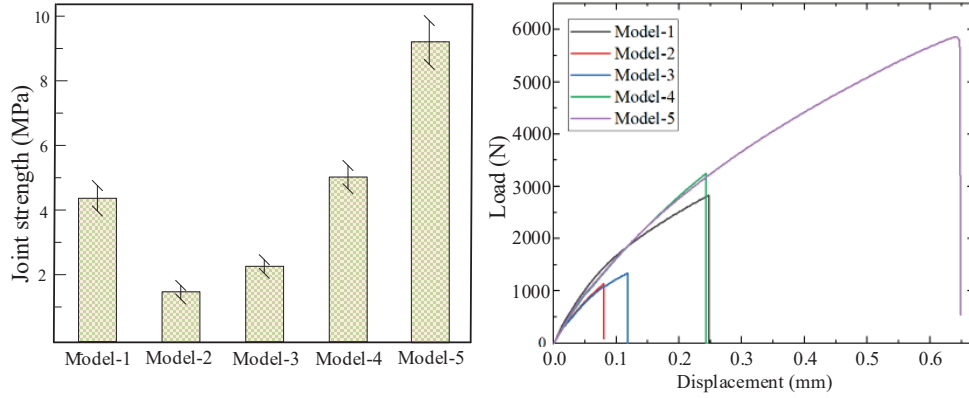


Fig.8. SLJs test results, (a) average shear strength of various SLJs, and (b) representative load-displacement curves.

On the other hand, in contrast to NaCl solution, the specimens treated with NaNO_3 solution not only failed to yield positive results but also resulted in a notable reduction in the bonding strength. Compared with Model-1, the average load of the Model-2 and Model-3, which had undergone electrochemical treatment in NaNO_3 solution, exhibited a notable decline, reaching approximately 1176 N and 1382 N, respectively. This phenomenon may be attributed to the continued adsorption of electrochemical treatment products on the aluminum substrate surface in NaNO_3 solution, leading to the formation of a corrosion layer. This hypothesis is supported by the findings presented in Sections 3.1 and 3.2. The corrosion layer adsorbed on the surface of the aluminum substrate has poor bonding strength with the aluminum substrate material, and is easily fracture during the loading process. This can be regarded as the primary cause of the notable reduction in the bonding performance of Model-2 and Model-3 in this section.

3.6 Failure mode analysis

The typical failure modes of SLJs and the SEM images of fracture surfaces are presented in Fig. 9. It can be clearly seen that Models 1-4 mainly experienced adhesive failure (as shown in Fig. 9(a)-(d)), while Model-5 clearly experienced mixed failure (as shown in Fig. 9(e)). For the purposes of analysis, the adhesive side is placed on the left (as shown in Fig. 9(f)-(i)), and the metal side is placed on the right (as shown in Fig. 9(k)-(n)). Model-5 experienced mixed failure, resulting in adhesive on both sides, and is therefore randomly placed (as shown in Fig. 9(j) and (o)).

Fig. 9(a) shows the typical failure model of SLJs made from untreated specimens.

The SEM images show that many adhesive residues can be seen on the metal surface (Fig. 9(k)). At the same time, there is no obvious replication of the initial texture on the adhesive surface (Fig. 9(f)), and the microfracture morphology is extremely heterogeneous. This phenomenon can be attributed to the poor hydrophilicity of the untreated specimen surface, as illustrated in Fig. 7. Consequently, the adhesive is unable to achieve complete penetration into the initial surface texture of the untreated specimen during the joint bonding process. In instances where the adhesives that penetrate into the initial texture are adhered to the metal surface due to the stronger mechanical locking effect. Conversely, the adhesives that are unable to penetrate the initial texture will be the first to fail during the loading process due to the infiltration of bubbles, which causes interfacial failure. The results of the fracture surface EDX analysis are presented in Table 7, which was employed to illustrate the alterations in the composition of the metal and adhesive surfaces. The Al content on the adhesive surface of the Model-1 is minimal, comprising only 0.15 wt % (Table 7(a)). This observation suggests that the initial oxide layer on the surface of the untreated specimen is firmly attached to the aluminum substrate. It can thus be proposed that the interfacial failure of Model-1 occurs at the contact interface between the adhesive and the initial oxide layer of the untreated surface.

Fig. 9(b) and (c) show the typical failure mode of SLJs made from specimens treated in NaNO₃ solution. It is noteworthy that the morphology of the metal surface following the failure exhibited a marked change from that observed prior to bonding. Compared with the surface morphology prior to bonding (Fig. 4(b)), the surface texture of the metal surface of Model-2 as shown in Fig. 9(l) has been disrupted, while the adhesive surface as shown in Fig. 9(g) displays some heterogeneous tissues that do not belong to the adhesive. Furthermore, compared with the markedly low Al content observed on the adhesive surface of Model-1, the Al content on the adhesive surface of Model-2 exhibited a notable increase, reaching 11.13 Wt%. This suggests that the heterogeneous tissues that has been adhered to the adhesive surface may be the corrosion products that was initially adsorbed on the surface of the aluminum substrate. This corrosion products were generated during the electrochemical treatment process

in a NaNO_3 solution. This provides a satisfactory explanation and evidence for the notable decline in the bonding performance of the Model-2 illustrated in Fig. 8. In other words, the corrosion products adsorbed on the surface of the aluminum substrate have a markedly deleterious effect on the bonding performance between the adhesive and the aluminum substrate.

On the other hand, the morphology of the metal surface of Model-3 has undergone a significant alteration from that observed prior to bonding. The corrosion layer that was present on the specimen surface prior to bonding in Fig. 4(c) has been entirely eliminated, as evidenced by the metal surface in Fig. 9(m). The elemental analysis of the adhesive surface depicted in Table 7 reveals a notable increase in the Al content of the adhesive surface in Model-3, when compared to the Al content of the adhesive surface in Model-1 and Model-2. The Al content of the adhesive surface in Model-3 has increased significantly, reaching 36.89 Wt%. This indicates that the corrosion layer that had adhered to the surface of the aluminum substrate, was completely stripped and adhered to the adhesive surface after the failure of the joint. It can thus be concluded that the failure of the Model-3 occurs at the bonding interface between the corrosion layer and the aluminum substrate. This is entirely distinct from the interface fracture properties of Model-1 and Model-2, which occur at the bonding interface between the adhesive and the initial oxide layer.

Fig. 9(d) and (e) show the typical failure models of SLJs made from the specimens treated in NaCl solution. Compared with the surface morphology prior to bonding as shown in Fig. 4(d) and (e), the metal surface morphology of Model-4 and Model-5 as shown in Fig. 9(n) and (o) also exhibited considerable alterations following failure. The elemental analysis presented in Table 7(d) and (e) demonstrates a notable increase in the elemental C content of the metal surfaces, which exceeds 70 Wt% following the SLJs failure. This indicates that the alteration in the morphology of the metal surfaces in Model-4 and Model-5 following failure is attributable to a substantial quantity of adhesive material being bonded to the metal surfaces. This is markedly distinct from the underlying causes of the alteration in metal surface morphology following failure in Model-2 and Model-3, which can be attributed to the stripping of processing products

or corrosion layers that adhered to the specimen surface during electrochemical treatment process. On the other hand, the Al content on the adhesive surface of Model-4 and Model-5 following failure also showed significant reduction, reaching approximately 5 Wt%, in comparison to the Al content on the adhesive surface of Model-2 and Model-3 after failure. This also corroborates the findings presented in [Sections 3.1 and 3.2](#), namely that the electrolyte solution exerts a significant influence on the surface morphology and composition of the electrochemical treated specimens. The corrosion products are more prone to adsorbing on the surface of the aluminum substrate in a NaNO₃ solution. Conversely, in a NaCl solution, almost no electrochemical corrosion products are adsorbed on the surface of the aluminum substrate.

Table 7

EDX elemental analysis of fracture surfaces of different models.

Element Samples		Adhesive side				Metal side			
		C	O	Al	Other	C	O	Al	Other
(a)	Wt%	80.50	16.28	0.15	3.07	19.72	2.75	75.67	1.86
	At%	85.76	13.02	0.07	1.15	35.05	3.68	59.88	1.39
(b)	Wt%	51.64	32.80	11.13	4.43	8.32	3.48	87.12	1.08
	At%	62.32	29.72	5.98	1.98	16.58	5.21	77.29	0.92
(c)	Wt%	20.65	37.2	36.89	5.26	5.84	4.63	89.54	-
	At%	31.06	42.00	24.76	2.18	11.87	7.07	81.06	-
(d)	Wt%	69.79	15.69	6.04	8.48	70.52	16.57	12.31	0.6
	At%	79.48	13.41	3.06	4.05	79.53	14.02	6.18	0.27
(e)	Wt%	57.43	20.12	4.78	17.67	72.33	19.64	6.45	1.59
	At%	73.73	19.39	2.73	4.15	79.88	16.29	3.17	0.66

Furthermore, compared with Model-1, Model-4 has more adhesive residue on the metal surface, which can be considered as the reason why Model-4 has higher bonding performances than Model-1, as shown in [Fig. 8](#). The previous test results in [Sections 3.2, 3.3 and 3.4](#) provide a good explanation for this phenomenon. Despite the similar surface roughness of the aluminum specimens of Model-1 and Model-4 before bonding ([Table 5](#)), the aluminum specimen of Model-4 exhibits a greater quantity of aluminum hydroxide as a result of the electrochemical treatment ([Fig. 6](#)). This has the effect of markedly enhancing the surface wettability ([Fig. 7](#)), leading to the higher bonding

performances for Model-4 in comparison to Model-1 (Fig. 8). Nevertheless, due to the low current density and the brief treated period, the surface morphology and composition of the specimens following electrochemical treatment exhibit minimal deviation from the untreated surface, as illustrated in Figs. 4 and 6. It can be proposed that the surface properties of aluminum specimens subjected to electrochemical treatment at low current remain basically unchanged, and the initial oxide layer persists to a large extent. Therefore, it can be posited that the adhesive failure situation of Model-4 is analogous to that of Model-1, occurring at the bonding interface between the adhesive and the initial oxide layer.

Compared with other SLJs, the failure of Model 5 is characterized by a shift from adhesive failure to mixed failure (Fig. 9(e)). This observation suggests that the bonding strength of the interface between the adhesive and the aluminum specimen has been markedly enhanced in Model-5. This phenomenon can be attributed to a number of factors. Firstly, the electrochemical treated specimen of Model-5 has the largest surface roughness of S_a 4.052 μm compared to the other specimens (Table 5), which results in a significant increase in the interfacial expansion area ratio (S_{dr}) from 37.082% of the untreated surface to 69.185%. This indicates that the electrochemical treated specimen of Model-5 resulted in an increase of over 80% in the actual bonding area expansion of the SLJs in comparison to the untreated surface. Secondly, the morphology and composition of the electrochemical treated specimen in Model-5 also underwent considerable alterations with the untreated surface. This indicates that the native oxide layer on the untreated surface has been entirely eliminated, as discussed in Sections 3.1 and 3.2. Furthermore, a new stable oxide layer with better wettability is formed on the surface of the aluminum substrate, effectively enhanced the expansion effect caused by the increase in surface roughness. In conclusion, the bidirectional enhancement of surface wettability and roughness provides the Model-5 with the optimal bonding performance.

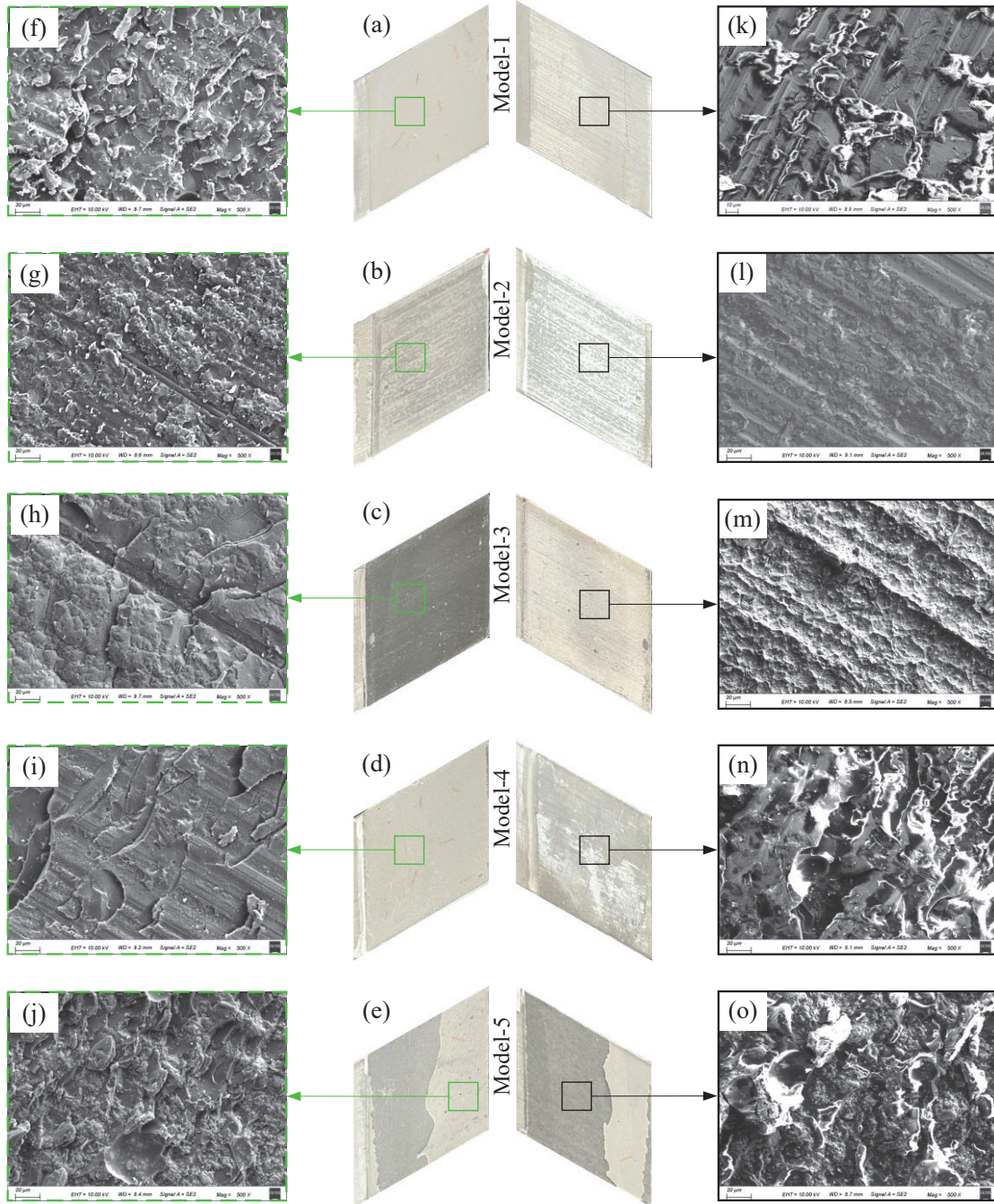


Fig. 9. Photographs and SEM images of fracture surfaces of different models, (a)-(e) photographs of fracture surfaces for Models 1-5, (f)-(j) SEM images of adhesive side, and (k)-(o) SEM images of metal side.

4. Fracture mechanisms of different SLJs

Based on the above test results and analysis, schematic diagrams of the fracture mechanisms of the five SLJs are established, as shown in Fig. 10. Each schematic consists of adhesive, native oxide/corrosion/stable oxide layer, aluminum substrate and two of its interfaces. The color gradient is employed to illustrate the alterations in

bonding strength. The color red is used to represent robust adhesion, whereas blue is used to represent its inverse. Fig. 10(a) and (f) illustrate the bonding and failure diagrams of the Model-1 joint, respectively. Due to the lack of electrochemical treatment, there are significant initial textures on the surface of the untreated specimen, and the native oxide layer is tightly adhered to the aluminum substrate. The native oxide layer displays poorly wettability and surface energy, which results in a markedly inferior bonding strength at interface 1 of the adhesive-native oxide layer in comparison to the interface 2 of the native oxide layer- aluminum substrate. Consequently, failure of the SLJs ultimately occurs at the interface 1 between the adhesive and the native oxide layer in the Model-1.

Fig. 10(b) and (g) show the bonding and failure diagrams of the Model-2 joint, respectively. Given the low current of 1A and brief treated period of 1 minute, the initial texture and native oxide layer of the untreated surface exhibit minimal alteration. However, the corrosion products generated during the electrochemical treatment process in the NaNO_3 solution tend to adhere to the surface of the native oxide layer, thereby significantly impairing the bonding performance at interface 1 of the adhesive-native oxide layer. Consequently, the bonding performance of Model-2 exhibited a markedly decline, reaching a level that was less than one-third of that observed for Model-1 (Fig. 8).

Fig. 10(c) and (h) show the bonding and failure diagrams of the Model-3 joint, respectively. Under high current conditions of 5A, the native oxide layer on the untreated surface was entirely removed, and the initial texture was also smoothed in NaNO_3 solution through electrochemical treatment. However, due to the accumulation of electrochemical treatment products, a corrosion layer was formed on the surface of the aluminum substrate in NaNO_3 solution. While the surface wettability of the electrochemical treated specimen was markedly enhanced, the bonding strength of the Model-3 joint was also considerably diminished as a consequence of the substantial reduction in the corrosion layer and aluminum substrate bonding strength. Ultimately, the failure occurred at the weaker interface 2 of the corrosion layer-aluminum substrate.

Fig. 10(d) and (i) illustrate the bonding and failure diagrams of the Model-4 joint,

respectively. Due to the low current of 1 A, the initial texture of the untreated surface was hardly removed. However, the higher corrosiveness of chloride ions ensured that the corrosion products generated during the electrochemical treatment process in NaCl solution would not adhere to the surface of the aluminum substrate. The bonding performance between the adhesive and the aluminum substrate was not only maintained but also enhanced as a consequence of the improved wettability resulting from the electrochemical treatment. However, due to the higher bonding strength at interface 2 of the native oxide layer- aluminum substrate, failure still occurs at the interface 1 of the native oxide layer-adhesive.

Fig. 10(e) and (j) illustrate the bonding and failure diagrams of the Model-5 joint, respectively. As a consequence of the considerable rise in the current to 5A, the initial texture of the untreated surface was effectively dissolved, resulting in the formation of a very rougher surface. This leads to a significant increase in the expansion area, which has a positive impact on bonding performance. On the other hand, due to the high corrosiveness of chloride ions, the native oxide layer on the untreated surface was entirely removed within 1 minute, and a new stable oxide layer was formed on the surface of the aluminum substrate. Thanks to electrochemical treatment in NaCl solution, this newly formed oxide layer contains more aluminum hydroxide, which has better wettability. This facilitates the penetration of the adhesive into the newly generated rough surface, thereby ensuring optimal adhesion. Finally, due to the combined enhancement effect of surface wettability and roughness, the bonding strength of interface 1 of the newly stable oxide layer-adhesive exceeded the adhesive strength, resulting in mixing failure.

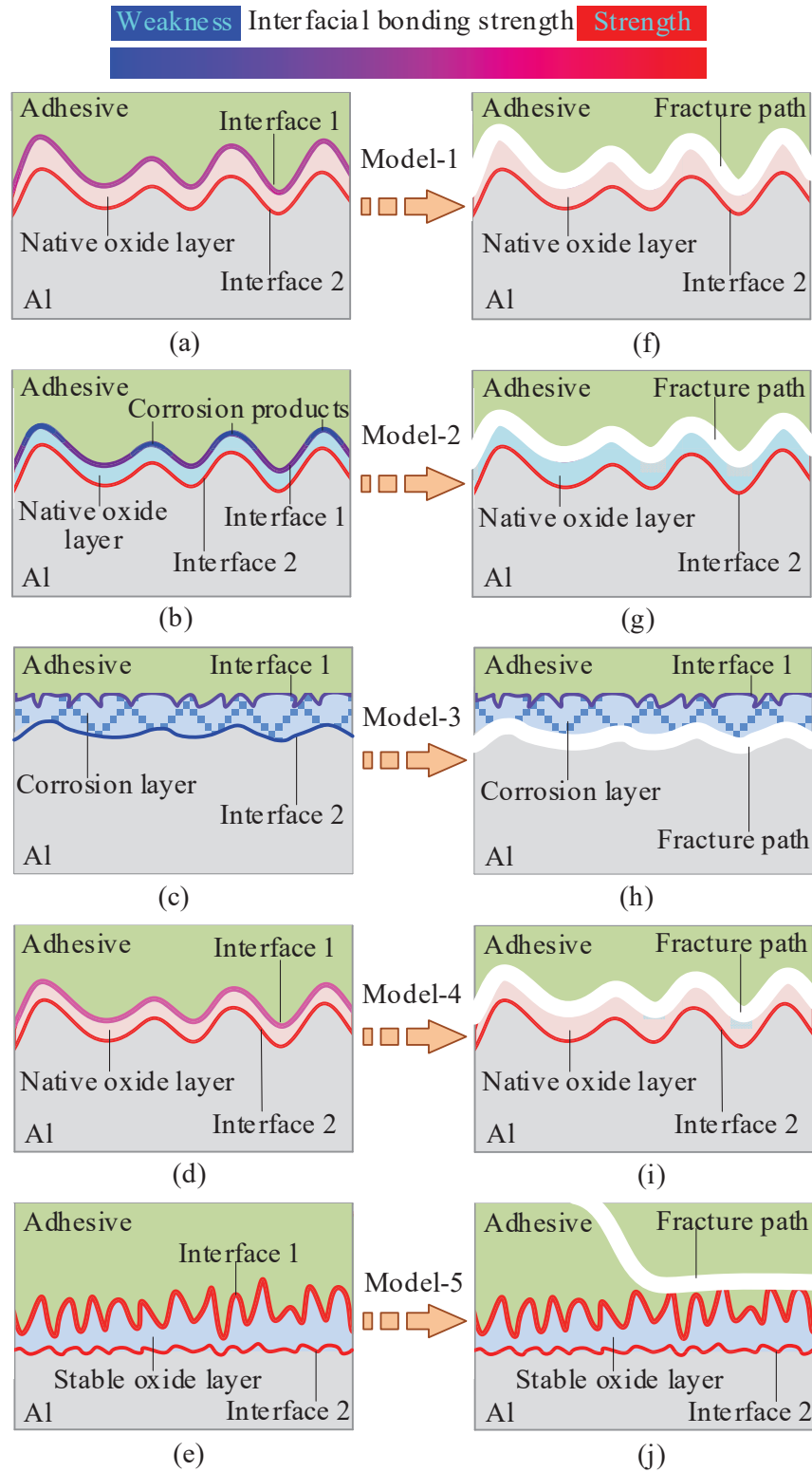


Fig.10. Schematic diagrams of the fracture mechanisms for different SLJs, (a)-(e) bonding diagram of Models 1-5, and (f)-(j) failure diagram of Models 1-5.

5. Conclusion

This paper presents the preliminary development of a novel electrochemical pretreatment for enhanced mechanical strength of adhesive aluminum joints using eco-

friendly neutral salt solution. A variety of characterization techniques were employed to observe alterations in the properties of aluminum alloy before and after electrochemical treatment, and detailed testing and analysis were also conducted on SLJs under different conditions. The conclusions are outlined as follows:

(1) The efficacy of electrochemical treatment in neutral salt solution as a means of enhancing the bonding performance has been demonstrated through experimental evidence. The method offers several technical advantages, including low cost, high efficiency, good bonding performance and environmental friendliness, which may make it an attractive option for many applications.

(2) The use of NaNO_3 solution has been found to have a detrimental effect on the bonding strength, due to the formation of electrochemical products which tend to adhere to the aluminum substrate surface during the electrochemical treatment process. These products can take the form of pollutants or corrosion layers, which damage the bonding performance between the adhesive and the aluminum specimen.

(3) The use of NaCl solution has been found to have a positive effect on the bonding strength. Due to the high corrosiveness of chloride ions, the electrochemical products are unlikely to adhere to the aluminum substrate surface. Furthermore, following the removal of the native oxide layer, a new stable oxide layer can be readily formed on the aluminum substrate, which exhibits better hydrophilicity.

(4) The improvement in bonding strength under NaCl solution and 1A is not significant due to the lack of sufficient electrochemical activity. While the application of NaCl solution and 5A results in the formation of a very rough surface with a larger expansion area on the aluminum substrate surface. The bonding strength was enhanced by over 200% in comparison to the untreated specimen, as a consequence of the combined effect of wettability and roughness.

Acknowledgment

This work was financially supported by the Jiangsu Agricultural Science and Technology Innovation Fund (CX(21)3154), the National Natural Science Foundation of China (52175438).

Credit Authorship Contribution Statement

Zhenghui Ge: Methodology, Investigation, Writing - Review & Editing. Qifan Hu: Investigation, Writing - Original Draft. Kai Pang: Investigation, Writing – Review & Editing. Yongwei Zhu: Methodology, Investigation, Writing - Review & Editing, Xiaonan Hou: Supervision, Writing - Review & Editing.

Reference

- [1] Szymiczek M, Chmielnicki B. Influence of epoxy resin curing systems and aluminium surface modification on selected properties of adhesive joints. *Pol J Chem Technol* 2018;20:26–31. <https://doi.org/10.2478/pjct-2018-0050>.
- [2] Hu Y, Zhang J, Wang L, Jiang H, Cheng F, Hu X. A simple and effective resin pre-coating treatment on grinded, acid pickled and anodised substrates for stronger adhesive bonding between Ti-6Al-4V titanium alloy and CFRP. *Surf Coat Tech* 2022;432:128072. <https://doi.org/10.1016/j.surfcoat.2021.128072>.
- [3] Wang H, Gao C, Chen Y, Wu M, Hua L. Ultrasonic Vibration-Strengthened Adhesive Bonding of CFRP/Aluminum Alloy Joints with Anodizing Pretreatment. *JOM-US* 2020;72:3472–82. <https://doi.org/10.1007/s11837-020-04284-4>.
- [4] Joo S, Yu M, Kim W S, Lee J, Kim H. Design and manufacture of automotive composite front bumper assemble component considering interfacial bond characteristics between over-molded chopped glass fiber polypropylene and continuous glass fiber polypropylene composite. *Compos Struct* 2020;236:111849–111849. <https://doi.org/10.1016/j.compstruct.2019.111849>.
- [5] Pereira BA, Fernandes AF. Sandwich Panels Bond with Advanced Adhesive Films. *J Compo Sci* 2019;3(3):79-79. <https://doi.org/10.3390/jcs3030079>.
- [6] Balakrishnan SV, Seidlitz H. Potential repair techniques for automotive composites: A review. *Compos Part B-Eng* 2018;145:28–38. <https://doi.org/10.1016/j.compositesb.2018.03.016>.
- [7] Robaidi AA, Anagreh N, Massadeh S, Essa AMA. The Effect of Different Surface Pretreatment Methods on Nano-adhesive Application in High Strength Steel and Aluminum Bonding. *J Adhes Sci Technol* 2011;25:1725–46. <https://doi.org/10.1163/016942410X535046>.
- [8] Rudawska A, Wahab M, Muller M. Strength of Epoxy-Bonded Aluminium Alloy Joints after Sandblasting. *Adv Science Technol-Res* 2022;16:262–79. <https://doi.org/10.12913/22998624/147524>.
- [9] Seo DW, Yoon HC, Lee JY, Lim JK. Effects of Surface Treatment and Loading Speed on Adhesive Strength of Aluminum to Polycarbonate Lap Joints. *Key engineering materials* 2004;261–263:405–10. <https://doi.org/10.4028/www.scientific.net/KEM.261-263.405>.
- [10] Valenza A, Fiore V, Fratini L. Mechanical behaviour and failure modes of metal to composite adhesive joints for nautical applications. *Int J Adv Manuf Tech* 2011;53:593–600. <https://doi.org/10.1007/s00170-010-2866-1>.
- [11] Wan H, Lin J, Min J. Effect of laser ablation treatment on corrosion resistance of adhesive-bonded Al alloy joints. *Surf Coat Tech* 2018;345:13–21. <https://doi.org/10.1016/j.surfcoat.2018.03.087>.
- [12] Zou X, et al. Laser surface treatment to enhance the adhesive bonding between steel and CFRP: Effect of laser spot overlapping and pulse fluence. *Opt Laser Technol* 2023;159:109002. <https://doi.org/10.1016/j.optlastec.2022.109002>.

- [13] Xu Z, Yip W, Dong Z, Uddin M, Stevens G. On the laser surface pre-treatment to enhance the surface texture, wettability and adhesion bonding strength of aluminium 7075-T6 laminates. *Compos Interface* 2024;31:123–41. <https://doi.org/10.1080/09276440.2023.2235804>.
- [14] Wang X, Lin J, Min J, Wang PC, Sun C. Effect of atmospheric pressure plasma treatment on strength of adhesive-bonded aluminum AA5052. *The J Adhes* 2018;94:701–22. <https://doi.org/10.1080/00218464.2017.1393747>.
- [15] Shin Y, et al. Significant slowdown of plasma-optimized surface energy deactivation by vacuum sealing for efficient adhesive bonding. *Compos Part B-Eng* 2022;240:110001. <https://doi.org/10.1016/j.compositesb.2022.110001>.
- [16] Dong X, Liu J, Hao H, Xue Y, Xu L. Effects of Different Surface Treatment Processes on Bonding Properties of Aluminum Alloys under Full Temperature Field Environment. *Crystals* 2023;13:1240. <https://doi.org/10.3390/cryst13081240>.
- [17] Gulcicek E, Diler EA, Ertugrul O. Synergistic effect of surface treatment and adhesive type on bonding performance of thin Al6061 joints for automotive applications. *Int J Adhes Adhes* 2024;130:103641. <https://doi.org/10.1016/j.ijadhadh.2024.103641>.
- [18] Konstantakopoulou M, Kotsikos G. Effect of MWCNT filled epoxy adhesives on the quality of adhesively bonded joints. *Plast Rubber Compos* 2016;45:166–72. <https://doi.org/10.1080/14658011.2016.1165788>.
- [19] Spadaro C, Dispenza C, Sunseri C. Influence of nanoporous structure on mechanical strength of aluminium and aluminium alloy adhesive structural joints. *J Phys-Condens Mat* 2006;18:S2007–18. <https://doi.org/10.1088/0953-8984/18/33/S16>.
- [20] Kadleckova M, et al. Preparation of Textured Surfaces on Aluminum-Alloy Substrates. *Materials* 2018;12:109. <https://doi.org/10.3390/ma12010109>.
- [21] Hu Y, Yuan B, Cheng F, Hu X. NaOH etching and resin pre-coating treatments for stronger adhesive bonding between CFRP and aluminium alloy. *Compos Part B-Eng* 2019;178:107478. <https://doi.org/10.1016/j.compositesb.2019.107478>.
- [22] Saleema N, Sarkar DK, Paynter RW, Gallant D, Eskandarian M. A simple surface treatment and characterization of AA 6061 aluminum alloy surface for adhesive bonding applications. *Appl Surf Sci* 2012;261:742–8. <https://doi.org/10.1016/j.apsusc.2012.08.091>.
- [23] Ali MT, Jebri Z, Jumel J. An enhanced surface treatment for effective bonding of 7075-T6 aluminium alloys. *J Adhesion* 2024:1–17. <https://doi.org/10.1080/00218464.2024.2321263>.
- [24] Prolongo SG, Urena A. Effect of surface pre-treatment on the adhesive strength of epoxy–aluminium joints. *Int J Adhes Adhes* 2009;29:23–31. <https://doi.org/10.1016/j.ijadhadh.2008.01.001>.
- [25] Shokrian MD, Shelesh-Nezhad K, Najjar R. The effects of Al surface treatment, adhesive thickness and microcapsule inclusion on the shear strength of bonded joints. *Int J Adhes Adhes* 2019;89:139–47. <https://doi.org/10.1016/j.ijadhadh.2019.01.001>.
- [26] Kang G, Choi W. A Study on the Effects of Surface Energy and Topography on the Adhesive Bonding of Aluminum Alloy. *Korean J Met Mater* 2021;59:567–74. <https://doi.org/10.3365/KJMM.2021.59.8.567>.
- [27] Pereira AM, Ferreira JM, Antunes FV, Bartolo PJ. Study on the fatigue strength of AA 6082-T6 adhesive lap joints. *Int J Adhes Adhes* 2009;29:633–8. <https://doi.org/10.1016/j.ijadhadh.2009.02.009>.
- [28] Zhang J, Zhao X, Zuo Y, Xiong J. The bonding strength and corrosion resistance of aluminum

- alloy by anodizing treatment in a phosphoric acid modified boric acid/sulfuric acid bath. *Surf Coat Tech* 2008;202:3149–56. <https://doi.org/10.1016/j.surfcoat.2007.10.041>.
- [29] Chen J, et al. Influence of surface microstructure on bonding strength of modified polypropylene/aluminum alloy direct adhesion. *Appl Surf Sci* 2019;489:392–402. <https://doi.org/10.1016/j.apsusc.2019.05.270>.
- [30] Dong L, Li Y, Huang M, Hu X, Qu Z, Lu Y. Effect of anodizing surface morphology on the adhesion performance of 6061 aluminum alloy. *Int J Adhes Adhes* 2022;113:103065. <https://doi.org/10.1016/j.ijadhadh.2021.103065>.
- [31] Critchlow GW, Yendall KA, Bahrani D, Quinn A, Andrews F. Strategies for the replacement of chromic acid anodising for the structural bonding of aluminium alloys. *Int J Adhes Adhes* 2006;26:419–53. <https://doi.org/10.1016/j.ijadhadh.2005.07.001>.
- [32] V. F, F. DF, R. M, M. S, D. B, A. V. Effects of anodizing surface treatment on the mechanical strength of aluminum alloy 5083 to fibre reinforced composites adhesive joints. *Int J Adhes Adhes* 2021;108:102868. <https://doi.org/10.1016/j.ijadhadh.2021.102868>.
- [33] Correia S, Anes V, Reis L. Effect of surface treatment on adhesively bonded aluminium-aluminium joints regarding aeronautical structures. *Eng Fail Anal* 2018;84:34–45. <https://doi.org/10.1016/j.engfailanal.2017.10.010>.
- [34] Iclal AA. The effect of chemical etching and nanostructure additive epoxy coating technique on adhesion strength in aluminum joints bonded with nanostructure additive adhesive. *Int J Adhes Adhes* 2024;129:103584. <https://doi.org/10.1016/j.ijadhadh.2023.103584>.
- [35] Zhang J, et al. Reinforcement study of anodizing treatment with various temperatures on aluminum substrates for stronger adhesive bonding with carbon fiber composites. *Surf Coat Tech* 2023;462:129473. <https://doi.org/10.1016/j.surfcoat.2023.129473>.
- [36] Zuo S, et al. An effective micro-arc oxidation (MAO) treatment on aluminum alloy for stronger bonding joint with carbon fiber composites. *Compos Part A-Appl S* 2024;177:107919. <https://doi.org/10.1016/j.compositesa.2023.107919>.
- [37] Nasreen A, Bangash MK, Shaker K, Nawab Y. Effect of Surface Treatment on Stiffness and Damping Behavior of Metal-Metal and Composite-Metal Adhesive Joints. *Polymers-Basel* 2023;15:435. <https://doi.org/10.3390/polym15020435>.
- [38] Yang S, Wang Y, Yang X, Lu X, Li MV, Zhu X. Effect of softening of 6082-T6 aluminum alloy CMT welded joints on mechanical properties and fracture behavior. *J Manuf Process* 2024;124:1567-1582. <https://doi.org/10.1016/J.JMAPRO.2024.07.046>.
- [39] Sareekumtorn P, Chaideesungnoen S, Muangjunburee P, Oo HZ. The electrochemical corrosion performance of aluminum alloys grade 6082-T6 weld repair. *Mater Res Express* 2024;11(8):086512-086512. <https://doi.org/10.1088/2053-1591/AD6EE3>.
- [40] Ravi KK, Narayanan GR, Rana KP. Friction Stir Spot Welding of Al6082-T6/HDPE/Al6082-T6/HDPE/Al6082-T6 sandwich sheets: hook formation and lap shear test performance. *J Mater Res Technol* 2019;8(1):615-622. <https://doi.org/10.1016/j.jmrt.2018.05.011>.
- [41] Kanani YA, Hou X, Ye J. A novel dissimilar single-lap joint with interfacial stiffness improvement. *Compos Struct* 2020;252. <https://doi.org/10.1016/j.compstruct.2020.112741>.
- [42] Kanani YA, Liu Y, Hughes JD, Ye J, Hou X. Fracture mechanisms of hybrid adhesive bonded joints: effects of the stiffness of constituents. *Int J Adhes Adhes* 2020;102(102649). <https://doi.org/10.1016/j.ijadhadh.2020.102649>.
- [43] Liu X, Li Y, Lei L, Wang X. The effect of nitrate on the corrosion behavior of 7075-T651

- aluminum alloy in the acidic NaCl solution. *Materials and Corrosion* 2021;72:1478–87. <https://doi.org/10.1002/maco.202112280>.
- [44] Wan H, Min J, Lin J. Experimental and theoretical studies on laser treatment strategies for improving shear bonding strength of structural adhesive joints with cast aluminum. *Compos Struct* 2022;279:114831. <https://doi.org/10.1016/j.compstruct.2021.114831>.
- [45] Jagdheesh R, Garcia-Ballesteros JJ, Ocana JL. One-step fabrication of near superhydrophobic aluminum surface by nanosecond laser ablation. *Appl Surf Sci* 2016;374:2–11. <https://doi.org/10.1016/j.apsusc.2015.06.104>.
- [46] Krawiec H, Vignal V, Schwarzenboeck E, Banas J. Role of plastic deformation and microstructure in the micro-electrochemical behaviour of Ti–6Al–4V in sodium chloride solution. *Electrochim Acta* 2013;104:400–6. <https://doi.org/10.1016/j.electacta.2012.12.029>.
- [47] Zain NM, Ahmad SH, Ali ES. Effect of surface treatments on the durability of green polyurethane adhesive bonded aluminium alloy. *Int J Adhes Adhes* 2014;55:43–55. <https://doi.org/10.1016/j.ijadhadh.2014.07.007>.
- [48] Kubiak KJ, Wilson MCT, Mathia TG, Carval Ph. Wettability versus roughness of engineering surfaces. *Wear* 2011;271:523–8. <https://doi.org/10.1016/j.wear.2010.03.029>.
- [49] Liang Y, et al. Contributions of surface roughness and oxygen-containing groups to the interfacial shear strength of carbon fiber/epoxy resin composites. *Carbon* 2024;218:118683. <https://doi.org/10.1016/j.carbon.2023.118683>.
- [50] Akpınar S, Kars A, Bayramoglu S, Demiral M. The influence of combination of surface roughness and nanostructure of adhesive on the strength of adhesively bonded joints. *Int J Adhes Adhes* 2024;133:103743. <https://doi.org/10.1016/j.ijadhadh.2024.103743>.